Low-temperature photo-induced mass transfer in thin $As_{20}Se_{80}$ amorphous films

V. Takáts, M.L. Trunov, K. Vad, J. Hakl, D.L. Beke, Yu. Kaganovskii, S. Kökényesi

PII: S0167-577X(15)30394-3
DOI: http://dx.doi.org/10.1016/j.matlet.2015.08.040
Reference: MLBLUE19401

To appear in: *Materials Letters*

Received date: 3 August 2015
Accepted date: 6 August 2015

Cite this article as: V. Takáts, M.L. Trunov, K. Vad, J. Hakl, D.L. Beke, Yu. Kaganovskii and S. Kökényesi, Low-temperature photo-induced mass transfer i thin $As_{20}Se_{80}$ amorphous films, *Materials Letters* http://dx.doi.org/10.1016/j.matlet.2015.08.040

Low-temperature photo-induced mass transfer in thin $As_{20}Se_{80}$ amorphous films

V. Takáts[a], M. L. Trunov[b,c], K. Vad[a], J. Hakl[a], D. L. Beke[d], Yu. Kaganovskii[e*], and S. Kökényesi[f]

[a]*Institute for Nuclear Research, HAS, Bem sq. 18/c, 4026 Debrecen, Hungary*

[b]*Uzhgorod National University, Narodna sq. 3, 88000 Uzhgorod, Ukraine;*

[c]*Uzhgorod Scientific Technological Center of IIR NAS Ukraine, Zamkovi shody st. 4a, 88000 Uzhgorod, Ukraine*

[d]*Dept. of Solid State Physics, University of Debrecen, H-4010 Debrecen, Hungary*

[e]*Dept. of Physics, Bar-Ilan University, Ramat-Gan 52900, Israel*

[f]*Institute of Physics, University of Debrecen, H-4010 Debrecen, Hungary*

Abstract

We have detected that surface relief gratings (SRG) in amorphous chalcogenide films $As_{20}Se_{80}$ can be optically recorded at low temperature, such as 77 K. A diffusion mechanism of photo-induced (PI) mass transport is proposed. A driving force of PI mass transport is a lateral steady state electric field induced by light interference. The kinetics of PI SRG growth depends on temperature due to temperature dependence of PI diffusion coefficients and concentration of radiation defects. By comparison of low temperature kinetics with that at 300 K we estimated diffusion activation energy, which turned out 0.09 eV. We present a model that explains low diffusion activation energy.

Keywords: amorphous chalcogenide films, diffusion, photo-induced mass transport, surface relief gratings.

PACS codes: 42.70.Ce, 66.30.hh, 42.50.Ct, 66.30.-h

*Corresponding author.

E-mail: kagany@ biu.ac.il; phone: 972-3-531-7864; fax: 972-3-738-4054

1. Introduction

Photo-induced (PI) variation of surface profile in amorphous chalcogenide films (ACF) under band gap light was repeatedly studied last years [1-6] (mainly at room temperature), due to possible wide applications in integrated optics and non-linear optics. Amongst different peculiarities of PI mass transport, such as strong dependence of the kinetics on the light polarization and intensity, it was detected that it can occur even at very low temperatures (77 K) [7]. The kinetics of the PI patterning at 77 K, however, was not studied, so that a mechanism of patterning was not proposed.

In this paper we study (experimentally and theoretically) the kinetics of PI formation of surface relief gratings (SRG) at 77 K in comparison to that at 300 K. We propose a diffusion mechanism of the mass transport, estimate PI diffusion coefficients and migration energy.

2. Experiment

We used for our experiments ACF $As_{20}Se_{80}$, which was previously selected as one of the most efficient materials for relief recording among the large number of Se- and S-based glasses [8]. The 2 μm thick $As_{20}Se_{80}$ thin films were prepared by thermal evaporation on a glass substrate at 10^{-5} Pa. The kinetics of SRG formation was studied under illumination of $As_{20}Se_{80}$ films by two *p*-polarized beams of diode laser (wavelength is 660 nm). Intensity of each of the beams was I_0 = 1 W/cm^2 and in addition to the interfering beams, the samples were illuminated (from the other side) by *s*-polarized beam with the intensity I_s = 2 W/cm^2. As it was previously shown [3], additional *s*-polarized beam increases the rate of SRG formation. SRG recording, as well as measurements of optical transmission spectra were preformed in Janis ST-100 optical cryostat. A pure helium gas flow was obtained from evaporating helium liquid transferred from He-Dewar. The gas temperature was adjusted by setting the helium inlet orifice and feeding helium pressure. The temperature of the helium gas was monitored inside the cryostat with the built-in silicone diode temperature sensor with

Lakeshore 331S Temperature Controller. Vacuum system of the cryostat was operated with oil free pumps. The obtained optical spectra were recorded by Ocean Optics millisecond spectrophotometer. Data on the SRG profile variation were obtained by *in situ* measurements of diffraction efficiency η, which was measured in reflection mode using a violet laser beam (λ = 406 nm, P = 1 mW). The intensity of the first diffraction peak depends on the SRG amplitude, h, as [9] $\eta = RJ_1^2(2\pi h/\lambda)$ where R is the reflectivity, and J_1 is the Bessel function. The SRG profiles after optical recording were scanned in atomic force microscope (AFM).

2. Results

Optical transmission of as prepared samples was measured before illumination at different temperatures (Fig. 1). With decreasing temperature the absorption edge shifts towards shorter wavelengths reflecting well known gap widening, in good accordance with literature [10,11].

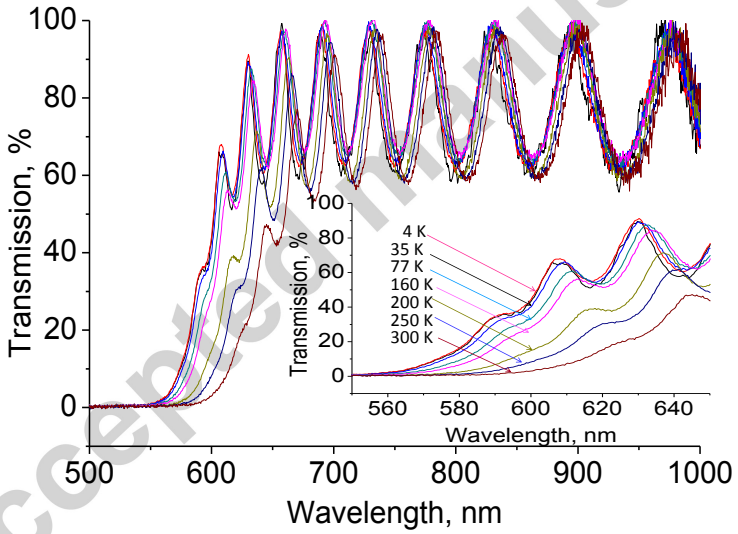

Fig. 1. Optical transmission spectra of as prepared $As_{20}Se_{80}$ films at various temperatures. In the inset one can see the temperatures used.

Under illumination by a laser beam (λ = 660 nm) transmission exponentially decreased with time due to photo-darkening. The characteristic time of the decrease varied from 152 s at 4 K to 416 s at 300 K, in agreement with the analysis [12] predicting exponential increase of density of radiation defects, responsible for photo-darkening. The rate of the defect accumulation is higher at lower temperature.

We recorded SRGs with the period Λ = 11 μm and compared the kinetics of the SRG amplitude growth at 77 K and 300 K (Fig. 2). As the absorption coefficient at 660 nm for 77 K is several times lower than that at 300 K, the samples before SRG recording at 77 K were illuminated by one of the beams to increase absorption due to photo darkening.

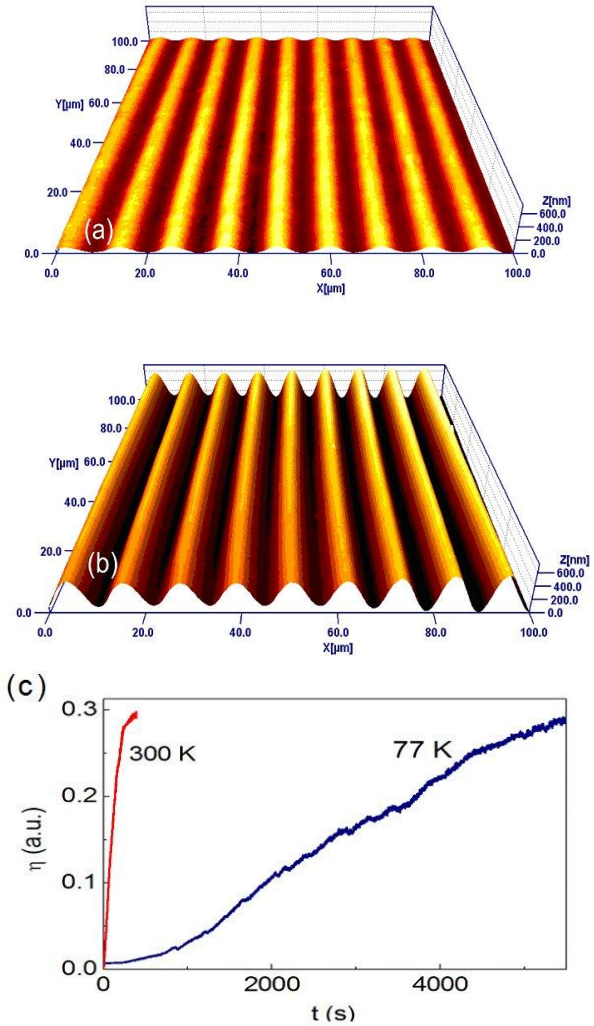

Fig. 2. AFM images of SRGs written at 77 K (a) and 300 K (b) at the same illumination conditions and $\eta(t)$ during recording of SRGs at 77 K and 300 K (c).

4. Discussion

Here, we propose a mechanism of PI mass transfer. Previously, several models were proposed to account for mass-transfer induced by light. All of them, however, based on the idea that the mass migration was driven by the electric field gradient of the polarized exciting light [1,3,4,13-17]. The field gradient moves dipolar defects (native and/or created by the

light) in a glass matrix softened by the lightening itself [2]. Existence of this driving force, however, suffers from difficulties (see, e.g., Ref. [18] for details). Moreover, quantitative estimates show that this mechanism is negligibly weak. Indeed, amplitude of electric field, E_l, associated with the light intensity, I, can be found from relation [19]

$$E_l^2 = (\mu_0 / \varepsilon_0)^{1/2} I / 2n_r \quad (1)$$

where n_r is refractive index, $\mu_0 = 4\pi \times 10^{-7}$ H/m is the vacuum permeability, $\varepsilon_0 = 8.85 \times 10^{-12}$ F/m is the vacuum permittivity. The dipole moment induced by the electric field of the light is $p = \alpha_e E_l$ (α_e is the electron polarizability, which is [20] 4.2×10^{-40} C m^2/V for Se atoms and 4.9×10^{-40} C m^2/V for As), and the force applied to the dipole is $F = \alpha_e E_l (\partial E_l / \partial x) \approx \alpha_e E_l^2 / \Lambda$. Substituting in Eq. (1) $I \approx 3 \times 10^7$ W/m^2 and $n_r = 2.45$ we find $E_l^2 \approx 2.3 \times 10^9$ V^2/m^2 and $F \approx 1 \times 10^{-26}$ N. Variation of energy due to a shift of the dipole in the field gradient for an interatomic distance $a \approx 2 \times 10^{-10}$ m is about 2×10^{-36} J that is negligible compared to average thermal energy even for 77 K ($kT \approx 1 \times 10^{-21}$ J).

Recently, a model was proposed [21] that allowed calculation of PI spatial and temporal profile evolution in ACF. According to the model, PI mass transport occurs by mechanism of viscous flow driven by optically induced pressure, $P_{opt} \approx \varepsilon_0 \varepsilon E_l^2$, which induces growth of the SRG amplitude (ε is dielectric constant of the ACF). Optical pressure, P_{opt}, competes with the Laplace pressure, $P_L = \gamma K \approx \gamma h / \Lambda^2$ (γ is the surface tension, K is the curvature) which has to smooth the forming profile. Numerical estimates show, however, that P_{opt} is very small compared to P_L and cannot be considered as a driving force of PI mass transfer. Indeed, with $E_l^2 \approx 2.3 \times 10^9$ V^2/m^2, $\varepsilon \approx 6$, $\gamma \approx 0.5$ J/m^2, $h \approx 100$ nm, and $\Lambda = 10$ μm, we have $P_{opt} \approx 0.12$ Pa, whereas $P_L \approx 5 \times 10^2$ Pa is three orders larger and should forbid the SRG formation.

Here, we propose a novel approach for the theoretical description of the mechanism of PI mass transfer in ACF. Our theoretical analysis is based on alternative driving force (in line with predictions and previous results [22,23]), namely, steady state lateral electric field, which appears in ACFs under non-homogeneous illumination by band gap light (Dember field [24]) due to different mobilities of generated electrons and holes. It is [25]

$$E(x) = -\frac{kT}{e} \cdot \frac{D_p - D_n}{p(x)D_p + n(x)D_n} \frac{dn(x)}{dx} \tag{2}$$

Here, e is the electron charge, $n(x)$, $p(x)$ and D_n and D_p are the local concentrations and the diffusion coefficients of electrons and holes. To satisfy the neutrality condition, one can suppose $n \approx p$. It is worth noting that existence of lateral steady state electric field under inhomogeneous illumination of $As_{20}Se_{80}$ film was recently demonstrated [23] using Kelvin probe force microscopy technique.

The steady state distribution of electrons, $n(x)$, can be found from the following differential equation [26]:

$$\frac{\partial n}{\partial t} = D_n \frac{\partial^2 n}{\partial x^2} - \frac{n}{\tau} + G(x) = 0 \tag{3}$$

Here, $G(x) = \alpha[2I_0(1+\cos qx) + I_s]/\chi E_g$ is the generation rate (number of electron-hole pairs created in unit volume per second), which is proportional to the absorbed light energy, α is the absorption coefficient, $2I_0(1+\cos qx)$ is the light intensity in the interference field created by two crossing beams in the x-direction, I_0 is the intensity created by each of the beams, I_s the intensity of additional s-polarized beam, $q = 2\pi/\Lambda$ is the wavenumber of forming grating, τ is the lifetime of PI electrons before recombination with holes, E_g is the band gap of the film material, and χ represents an efficiency factor that includes light energy losses due to scattering and phonon interactions.

Solution of Eq. (3) for periodic boundary conditions is

$$n(x) \approx \frac{2\alpha\Omega\tau\left[I_0 \cos qx + (1+q^2l^2)(I_0 + I_s/2)\right]}{(1+q^2l^2)\chi E_g} \tag{4}$$

Here, Ω is the average atomic volume in ACF, $l = \sqrt{D_n\tau}$ is the electron diffusion length. Taking into account Eq. (4) we obtain from Eq. (2)

$$E \approx \frac{kT \cdot \delta \cdot I_0 q \sin qx}{e\left[I_0 \cos qx + (1+q^2l^2)(I_0 + I_s/2)\right]} \qquad \delta = \frac{D_p - D_n}{D_p + D_n} \tag{5}$$

The amorphous $As_{20}Se_{80}$ used in our experiments is photoconductive *p*-type semiconductor with the atomic structure consisting mainly of chains with *C–C* and partly *P–C* bonds (*P* and *C* denotes pnictogen and chalcogen atoms, respectively). Previously we have shown [27] that the main mechanism of PI mass transfer is volume diffusion, in contrast to viscous flow. The diffusion coefficients are accelerated under irradiation due to creation of radiation defects, whose concentration, $n_{ex}(x)$, is proportional to $n(x)$ or $p(x)$. We assumed that $n_{ex}(x) = \xi\, n(x)$ with $\xi \approx 0.1$. As $D_p >> D_n$ in $As_{20}Se_{80}$, we assumed $\delta \approx 1$ both for 300 K and 77 K.

As it follows from the atomic theory of diffusion [28], the PI diffusion coefficients can be given as [22]

$$D_k = \frac{1}{2}\Gamma_k a^2 \approx \frac{1}{2} a^2 \nu_0 n_{ex} c_k e^{-Q_m^k/kT} \qquad k = P, C \tag{6}$$

Here, *a* is the average length of elementary jump, Γ_k is the jump frequency, which is determined by the probability of thermal activation nearby an existing defect, the product $n_{ex}c_k$ is the probability to meet a *k*-type of charged species near the free volume (radiation defect), c_k is the atomic concentration of *k*-type charged species, ν_0 is the frequency of atomic oscillations and Q_m^k is the migration energy.

The kinetics of SRG amplitude growth was calculated similarly to that made previously for electron beam induced mass transport [22]. We assumed that mobile species have an

effective charge, *e*, positive or negative, since electrons and holes are localized near radiation defects. Both *P* and *C* atoms can be charged either positively or negatively depending on localization of electrons or holes around them. Lateral diffusion flux was defined as a drift of the charged species in the lateral electric field [see Eq. (5)]

$$J_x \approx -\frac{D^- + D^+}{\Omega kT} eE \tag{7}$$

where $D^{\pm} = D_P^{\pm} c + D_C^{\pm}(1-c)$, c is atomic fraction of *P* atoms in the ACF, $D_P^{\pm}$ and $D_C^{\pm}$ are diffusion coefficients of *P* and *C* atoms with the localized holes or electrons. The positively and negatively charged *P* and *C* atoms should drift in opposite directions. The drift however does not change electro neutrality because electrons and holes diffuse much faster than the charged species and ensure neutrality of the film. According our numerical estimates,[22] the most mobile are P_2^- and C_1^- atoms ($D^- >> D^+$), so we neglected coefficients D^+ in Eq. (7) and used effective diffusion coefficient, $D \approx D_P^- c_P + D_C^-(1-c_P)$, which describes the mass transfer kinetics, in the form

$$D \approx \frac{1}{2} a^2 \nu_0 n_{ex} e^{-Q_m/kT} = D_0 n_{ex} e^{-Q_m/kT} \tag{8}.$$

where Q_m is effective migration energy and $D_0 \approx a^2 \nu_0 / 2$. Eq. (8) is valid if $c_P \exp(-\Delta Q_m / kT << 1$ (ΔQ_m is difference between the PI migration energies of *P* and *C* atoms).

The surface profile, *z*(*x*,*t*), and the normal rate of SRG growth can be given by

$$z(x,t) = h(t)\cos qx$$

$$\frac{\partial z}{\partial t} = -\Omega \cdot \left[H_0 + h(t)\cos qx\right] \cdot \frac{dJ_x}{dx} \tag{9}$$

Here, H_0 is the average film thickness. As it was previously shown [3,6,**Error! Bookmark not defined.**], under illumination of $As_{20}Se_{80}$ films by *p*-polarized beams with the low enough

intensities, the mass transfer is directed from dark to light regions and thus maxima of SRG correspond to maxima of the light intensity. As it follows from Eqs. (5), (7), and (9), $h(t)$ can be determined from equation

$$\frac{dh(t)}{dt} = A + Bh(t) \tag{10}$$

where $A = D\delta \cdot q^2 H_0 \Big/ \left[\cos qx + (1 + I_s / 2I_0)(1 + q^2 l^2)\right]$ and $B = A\cos qx / H_0$.

We neglect for simplicity capillary forces, which has to flatten the profile because, according to our estimates, capillary force ($\sim K\gamma\Omega/\Lambda$) for SRG period Λ = 11 μm is about three orders of magnitude smaller than the electrostatic force.

Solution of Eq.(10) with initial condition $h(0) = h_0$ is

$$h(t) = -\frac{A}{B} + e^{Bt}\left(h_0 + \frac{A}{B}\right) \tag{11}$$

If $h_0 << H_0$ and $Bt << 1$, $h(t)$ is close to linear dependence. In Fig. 3 we compare SRG amplitude, $h(t)$, calculated using Eq. (11) with experimental data shown in Fig. 2d [we transformed diffraction efficiencies $\eta(t)$ into $h(t)$]. For calculations we used parameters shown in Table 1. As fitting parameters, we took diffusion coefficients, D, and electron diffusion length, l, which are also shown in the Table I. The coefficient D estimated for 300 K is in agreement with the previously determined PI coefficients [27].

Table I. Parameters used for calculations

T, K	300	77
α, cm^{-1}	2.4×10^{3}	2.0×10^{3}
E_g, eV	2.01	2.15
l, μm	2.8	1.2
$n_{ex}(0)$	1.5×10^{-7}	1.9×10^{-4}
D, cm^2/s	1.0×10^{-10}	1.4×10^{-12}

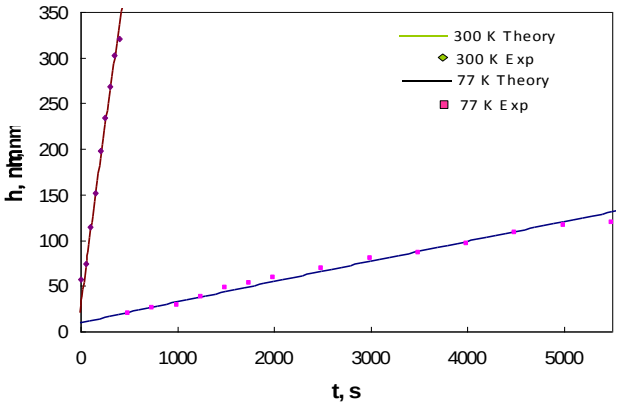

Fig. 3. Comparison of experimental and calculated $h(t)$ for 77 K and 300 K.

The effective migration energy Q_m and pre-exponent factor D_0 were estimated from Arrhenius plot for ratio D/n_{ex} [see Eq. (8)] using values shown for 77 K and 300 K in Table I. We obtained Q_m = 0.09 eV and D_0= 1.8×10^{-2} cm^2/s.

The low diffusion activation energy can be easily explained if we consider Coulomb interaction between charges localized near the radiation defects and bounded with the diffusing atom. Coulomb interaction deforms potential barrier for migration (see Fig. 4): quasi-periodic potential $U_0(r)$ with the initial migration barrier Q_{m0} transforms into $U(r) = U_0(r) + e^2/r$, and the migration barrier, Q_m, becomes very small near the radiation defect. Pre-exponential factor D_0 estimated from the kinetics of SRG formation, is in agreement with the atomic diffusion theory that predicts $D_0 \approx a^2\nu_0 \approx 10^{-2}$ cm^2/s (with $a^2 \approx 10^{-15}$ cm^2 and $\nu_0 \approx 10^{13}$ s^{-1}).

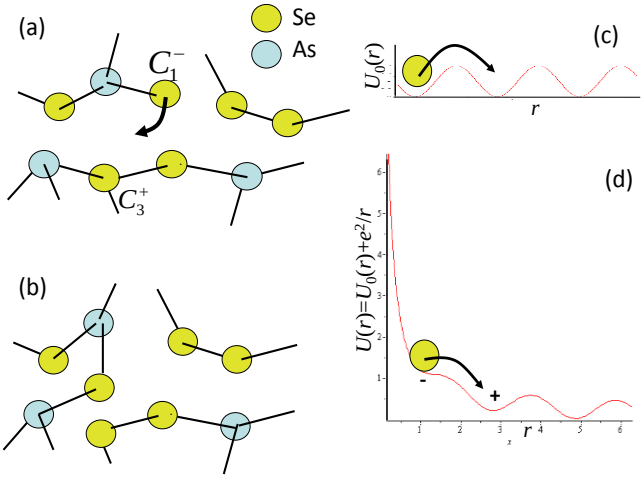

Fig. 4. Scheme of migration of Se atom with bounded electron into free volume produced by a radiation defect, which contains electron-hole pair (a). After migration, a new configuration is formed (b). Potential barrier for migration of neutral atom (c) can be noticeably deformed (d) due to Coulomb interaction of electron connected with the migrating atom and hole localized near the radiation defects.

5. Conclusions

We have measured and theoretically described the kinetics of low temperature PI mass transfer. We have proposed a driving force and a mechanism of the PI mass transfer, estimated the PI diffusion coefficients at 77 and 300 K, the diffusion migration energy, Q_m, and explained its low value.

Acknowledgements

This work was supported by the TAMOP 4.2.2.A-11/1/KONV-2012-0036 project, which is co-financed by the European Union and European Social Fund.

References

[1] Saliminia A, Galstian TV, and Villeneuve A. Phys Rev Lett: 2000; 85: 4112.

[2] Yannopoulos SN, and Trunov ML. Phys stat sol B: 2009; 246: 1773.

[3] Trunov ML, Lytvyn PM, Nagy PM, Dyachyns'ka OM. Appl Phys Lett: 2010; 97: 031905.

[4] Trunov ML, Lytvyn PM and Dyachyns'ka OM. Appl Phys Lett: 2010; 96: 111908.

[5] Kaganovskii Yu, Beke DL and Kökényesi S. Appl Phys Lett: 2010; 97: 061906.

[6] Kaganovskii Yu, Beke DL, Charnovych S, Kökényesi S, Trunov ML. J Appl Phys: 2011; 110: 063502.

[7] Poborchii VV, Kolobov AV and Tanaka K. Appl Phys Lett: 1999; 74: 215.

[8] Trunov ML, Nagy PM, Takats V, Lytvyn PM, Kokenyesi S, Kalman E. J Non-Cryst Solids: 2009; 355: 1993.

[9] Ratcliffe A. Rep Prog Phys: 1956; 19: 188.

[10] Tichý L, Tichá H, Nagels P, Callaerts R, Mertens R, Vlček M. Mater Lett: 1999; 39: 122.

[11] Nagels P, Tichý L, Mertens R, Callaerts R. Mater Lett: 2000; 46: 234.

[12] Kvangjoon K, Arthur JE. Appl Phys Lett: 1995; : 2786.

[13] Asatryan KE, Galstian T and Valle´e R. Phys Rev Lett: 2005; 94: 087401.

[14] Fritzsche H. Phys Rev B: 1995; 52: 15854.

[15] Kumar J, Li L, Li Jiang X, Kim D-Y, Seung Lee T, and Tripathy S. Appl Phys Lett: 1998;72: 2096.

[16] Tikhomirov VK. J Non-Cryst Solids: 1999; 256 & 257: 328.

[17] Tikhomirov VK, Asatryan K, Galstian TV, Vallee R and Seddon AB. Phil Mag Lett: 2003; 83: 117.

[18] Tanaka K and Asao H. Jpn J Appl Phys: 2006; 45: 1668.

[19] Boyd RW. *Nonlinear Optics*: 2003; Academic Press.

[20] *CRC Handbook of Chemistry and Physics*, 95th Edition: 2014; Ed. Haynes WH, CRC Press.

[21] Lu C, Recht D and Arnold C. Phys Rev Lett: 2013; 111: 105503.

[22] Trunov ML, Cserhati C, Lytvyn PM, Kaganovskii Yu and Kokenyesi S. J Phys D: Appl. Phys: 2013; 46: 245303.

[23] Trunov ML, Lytvyn PM, Nagy PM, Csik A, Rubish VM and Kökényesi S. Phys stat solidi B: 2014; 251: 1354.

[24] Dember H. Phys Zeits: 1931; 32: 554.

[25] Seeger K. *Semiconductor Physics*: 1985; Springer, Berlin.

[26] Thomas Ch, Joachimsthaler I, Heiderhoff R and Balk LJ. J Phys D: Appl Phys: 2004; 37: 2785.

[27] Kaganovskii Yu, Trunov ML, Beke DL and Kökényesi S. Mater Lett: 2012; 66: 159.

[28] Shewmon PG. *Diffusion in Solids* 2nd edn: 1989; Wiley, New York.

Highlights

Low temperature photo-induced mass transfer in amorphous chalcogenide films is detected.

The mass transfer kinetics is measured and theoretically described.

Photo-induced diffusion coefficients and activation energy are estimated.

Diffusion mechanism of the mass transfer is proposed that explains low migration energy.